

MOHIT LAL¹

MULTIPLE FAULT PARAMETER ESTIMATION OF A FULLY ASSEMBLED TURBOGENERATOR SYSTEM

The present article investigates the dynamic behavior of a fully assembled turbogenerator system influenced by misalignment. In the past, most of the researchers have neglected the foundation flexibility in the turbogenerator systems in their study, to overcome this modelling error a more realistic model of a turbogenerator system has been attempted by considering flexible shafts, flexible coupling, flexible bearings and flexible foundation. Equations of motion for fully assembled turbogenerator system including flexible foundations have been derived by using finite element method. The methodology developed based on least squares technique requires forced response information to quantify the bearing–coupling–foundation dynamic parameters of the system associated with different faults along with residual unbalances. The proposed methodology is tested for the various level of measurement noise and modelling error in the system parameters, i.e., 5% deviation in E (modulus of elasticity) and ρ (density), respectively, for robustness of the algorithm. In a practical sense, the condition analyzed in the present article relates to the identification of misalignment and other dynamic parameters viz. bearing and residual unbalance in a rotor integrated with flexible foundation.

1. Introduction

The most common turbogenerator system comprises the driver and driven shafts connected with coupling, mounted on bearings, and the complete system is laid on a flexible foundation. Such category of the dynamic system needs accurate as well as reliable prediction of its dynamic behavior of components and identification of impending faults associated with it.

To identify various faults present in turbogenerator systems such as residual unbalance, rotor cracks, shaft misalignments, gear faults etc., multiple techniques

¹Department of Industrial Design, National Institute of Technology Rourkela, India. Email: lalm@nitrkl.ac.in

have been developed [1–6] based on feature-based method (like fuzzy-logic, support vector machine, artificial neural network (ANN)). Due to incomplete information available with feature extraction methods, scholars and personnel working in this are moving towards more appropriate technique of identification, i.e., model-based technology. Model-based techniques not only classify the faults but also gives quantitative information regarding the various flaws present in the system.

Authors of [7] used higher-order finite element method to incorporate eight degrees of freedom per node. In this analysis, they modelled the faults as equivalent force system and obtained fault parameters numerically. Ref. [8] presented a method to calculate the force applied to the bearing by securing response at the bearing, and this information is further processed to estimate foundation parameters. The present method requires prior knowledge of unbalance. Also, this technique was demonstrated by using a simple rotor bearing model. They reported vibration responses corresponding to $2\times$ represents significant variations due to misalignment. A similar approach as used in [8] except using a Kalman filter to estimate the foundation parameters is used in [9]. Moreover, no experimental result was presented in this analysis.

Authors of [10] proposed a novel approach to take measurement that reduces the requirement of prior knowledge of the rotor bearing model. To check the accuracy of the developed algorithm considered frequency range was split into various frequency bands, and for each frequency band estimates were obtained. Articles [11, 12] presented a technique to include a modal model of foundation structure in the equations of motion (EOMs). The method shows that there were no constraints in the modelling of foundation structure. The identification algorithm developed in the frequency domain can be integrated with a modal model of the foundation. In this method, modal test is not required to estimate modal parameters. Phase modification and numerical optimization to improve the accuracy of foundation model is presented in [13]. Frequency response function was used to estimate the foundation parameters of the system, and it was concluded that implementation of pseudo mode shape method (PMSM) improves the accuracy of identification algorithm.

Authors of [14] reviewed the various methods of machine prognosis that forecast the operational life, future condition and probability of reliable operation of a component. They categorized multiple methods used for estimating rotating machinery fault as conventional reliability model, condition based prognostic model, and model integrating reliability and prognostics. Ref. [15] presented a method to evaluate the effect of supporting structure on a rotor bearing system by considering physical coordinate of the rotor bearing system and the principal coordinate of foundation a frequency response analysis of the whole operation was done. They used directional frequency response function to estimate the parameters and compared the results obtained with the conventional frequency response function procedure. An algorithm developed based on least squares fit to estimate multiple faults of a turbogenerator system is presented in [16]. They used an analytical approach, i.e.,

Lagrange's method to develop equations of motion. The accuracy of the developed algorithm is checked for the different level of measurement noise and modeling error. The aforementioned identification algorithm is extended for the more realistic model to estimate dynamic parameters of the turbogenerator system and a novel condensation scheme is proposed in [17]. Authors of [18] reviewed the various methods used in signal based condition monitoring technique and concluded that empirical mode decomposition technique (EDM) is one of the most powerful tools for rotor fault detection and diagnosis. Ref. [19] presented an approach to identify foundation parameters by equation decoupling method. In this analysis, they compared and reported fair agreement between the numerical simulation results with the ANSYS.

In this article, a more realistic turbogenerator model with the flexible foundation is considered, and its effect on the estimation of misalignment and other dynamic parameters of the turbogenerator system has been analyzed. A more practical approach, i.e., finite element method (FEM) is used to obtain system equations of motion (EOMs). To quantitatively estimate the dynamic parameters of the system a methodology has been developed based on least squares technique. To evaluate the correctness of the developed methodology measurement noise (up to 5%) has been considered. Moreover, modeling error, i.e., 5% deviation in E (modulus of elasticity) and ρ (density) has also been added for some physical parameters, and the algorithm is found to be robust.

2. Theoretical development

Assumptions involved in the modeling of the system and an approach to evaluate dynamic system parameters along with foundation parameters have been discussed in this section.

2.1. Model description

Schematic representation of the model considered in this analysis is shown in Fig. 1. The model consists of two flexible shafts connected with the help of flexible coupling, each shaft is mounted on two flexible bearings (anisotropic) at the ends and the fully assembled model is supported on a flexible foundation. Timoshenko beam theory is applied to model flexible shafts having mass (m^s) and diametral mass moment of inertia (I_d^s). Each shaft is having two rigid discs of mass (m_i^d), diametral mass moment of inertia (I_i^d) and the residual unbalance (u_i) where $i = 1, 2, 3, 4$. FEM is used to obtain mass, damping (Rayleigh's damping) and stiffness matrix of the shaft. The finite element (FE) model of system is shown in Fig. 2, each node is having four degrees of freedom (DOFs) i.e., two translational (x, y) and two rotational (φ_x, φ_y). Where B_i, D_i and F_i , ($i = 1, 2, 3, 4$) represents bearing, disc and foundation location, respectively. The foundation is modeled similar as bearings and having eight linearized stiffness $k_{ij}^{b_n}, k_{ij}^{f_n}$ and damping $c_{ij}^{b_n}, c_{ij}^{f_n}$ coefficients.

Subscripts i and j represent two orthogonal directions x and y . Superscripts b, d, f and s represent bearing, disc, foundation and shaft, respectively. While $n = 1, 2, 3, 4$ is used to represent number of bearings, disc and foundations. For brevity internal damping, gyroscopic effect is neglected and speed independent parameters are considered to develop identification algorithm in the present study.

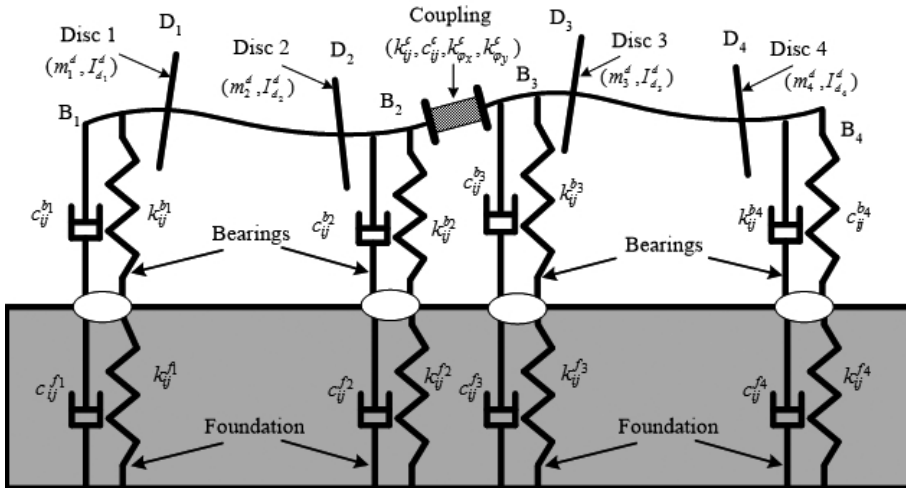


Fig. 1. A flexible rotor–bearing–coupling–foundation system

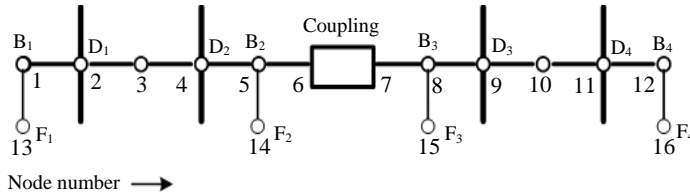


Fig. 2. Finite element model of flexible rotor–bearing–coupling–foundation system

2.2. Shaft and disc model

Flexible shafts and rigid discs are considered in this analysis. Shafts are modelled with the help of Timoshenko beam theory. The elemental mass $[M]$, stiffness $[K]$ and damping $[C]$ matrices for Timoshenko beam theory are well established in [20, 21]. Elemental EOMs of the shaft and disc could be expressed as

$$[M]^s \{\ddot{\eta}(t)\}^s + [C]^s \{\dot{\eta}(t)\}^s + [K]^s \{\eta(t)\}^s = \{f(t)\}^s \tag{1}$$

and

$$[M]^d \{\ddot{\eta}(t)\}^d = \{f(t)\}^d. \tag{2}$$

2.3. Rotor model

The rotor consists of two substructures namely shaft and disc. Elemental EOMs for rotor could be obtained by adding individual elemental EOMs of shaft and disc, i.e., Eq. (1) and (2), respectively and could be expressed as

$$[M]^R \{\ddot{\eta}(t)\}^R + [C]^R \{\dot{\eta}(t)\}^R + [K]^R \{\eta(t)\}^R = \{f(t)\}^R, \quad (3)$$

where

$$[M]^R = [M]^s + [M]^d; \quad [C]^R = [C]^s; \quad [K]^R = [K]^s \quad \text{and} \quad \{f\}^R = \{f\}^s + \{f\}^d.$$

2.4. Bearing and foundation model

Bearings and foundations are formulated with short bearing approximation theory and modeled as having eight linearized stiffness and damping coefficients. The elemental EOMs for each bearing and foundation could be written as

$$[C]^B \{\dot{\eta}(t)\}^B + [K]^B \{\eta(t)\}^B = \{f(t)\}^B \quad (4)$$

and

$$[C]^F \{\dot{\eta}(t)\}^F + [K]^F \{\eta(t)\}^F = \{f(t)\}^F. \quad (5)$$

Details of elemental matrices for bearing and foundation could be given as

$$[K]^B = \begin{bmatrix} k_{xx}^{b1} & k_{xy}^{b1} \\ k_{yx}^{b1} & k_{yy}^{b1} \end{bmatrix}; \quad [C]^B = \begin{bmatrix} c_{xx}^{b1} & c_{xy}^{b1} \\ c_{yx}^{b1} & c_{yy}^{b1} \end{bmatrix}$$

and

$$[C]^F = \begin{bmatrix} c_{xx}^{f1} & c_{xy}^{f1} \\ c_{yx}^{f1} & c_{yy}^{f1} \end{bmatrix}; \quad [K]^F = \begin{bmatrix} k_{xx}^{f1} & k_{xy}^{f1} \\ k_{yx}^{f1} & k_{yy}^{f1} \end{bmatrix}.$$

2.5. Coupling misalignment model

A flexible coupling consists of linear and torsional springs and linear dampers to accommodate combined misalignment effect into account are considered. The restoring and damping force has been included in stiffness and damping matrix. The amount of misalignment significantly depends upon the different modes of excitation and would reflect in term of damping and stiffness force during motion that will change with speed. The EOMs for coupling could be expressed as

$$[C]^c \{\dot{\eta}(t)\}^c + [K]^c \{\eta(t)\}^c = \{f(t)\}^c, \quad (6)$$

where superscript 'c' represents coupling. Details of the elemental matrix as well as misalignment forces and moments equations are taken from [16].

2.6. Residual unbalance force model

Residual unbalance force could be expressed as

$$\{f_{unb}(t)\} = \{F_{unb}(t)\}e^{j\omega t}, \quad (7)$$

where $\{F_{unb}(t)\}$ is complex residual unbalance force vector containing amplitude and phase information.

2.7. System equations of motion

The elemental EOMs of the rotor, bearing, foundation and coupling as sub-structure are presented in Eqs. (3)–(6), respectively. Force is expressed as shown in Eq. (7). Upon consideration of solution of Eqs. (3)–(6) as $\{\eta(t)\} = \{\bar{\eta}\}e^{j\omega t}$. The governing equation for rotor, bearing, foundation and coupling, respectively in frequency domain could be represented as

$$[Z_R]_{48 \times 48} \{\eta_R\}_{48 \times 1} = \{F_R\}_{48 \times 1}, \quad (8)$$

$$[Z_B]_{8 \times 8} \{\eta_B\}_{8 \times 1} = \{F_B\}_{8 \times 1}, \quad (9)$$

$$[Z_F]_{8 \times 8} \{\eta_f\}_{8 \times 1} = \{F_F\}_{8 \times 1} \quad (10)$$

and

$$[Z_C]_{8 \times 8} \{\eta_C\}_{8 \times 1} = \{F_C\}_{8 \times 1}. \quad (11)$$

Numbers shown at subscripts in the above equations represent the size of the respective matrices, where $[Z_R]$, $[Z_B]$, $[Z_F]$ and $[Z_C]$ are the dynamic matrix for the rotor, bearing, foundation and coupling, respectively. Details of these dynamic matrices are:

$$[Z_R]_{48 \times 48} = ([K_R] + j\omega[C_R] - \omega^2[M_R]), \quad (12)$$

$$[Z_B]_{8 \times 8} = ([K_B] + j\omega[C_B]), \quad (13)$$

$$[Z_F]_{8 \times 8} = ([K_F] + j\omega[C_C]) \quad (14)$$

and

$$[Z_C]_{8 \times 8} = ([K_C] + j\omega[C_C]). \quad (15)$$

All DOFs of the rotor system are divided into two parts, namely internal and connection DOFs. Linear DOFs at bearing as well as foundation and all DOFs at coupling (linear as well as angular) are considered as connection DOFs, whereas apart from these all, other DOFs are regarded as internal DOFs. Eqs. (12)–(15), are divided into connection and internal DOFs and it could be expressed as,

$$\begin{bmatrix} [Z_{R,II}] & [Z_{R,IB}] & [Z_{R,IC}] & [Z_{R,IF}] \\ [Z_{R,BI}] & [Z_{R,BB}] & [Z_{R,CC}] & [Z_{R,BF}] \\ [Z_{R,CI}] & [Z_{R,CB}] & [Z_{R,CC}] & [Z_{R,CF}] \\ [Z_{R,FI}] & [Z_{R,FB}] & [Z_{R,FC}] & [Z_{R,FF}] \end{bmatrix} \begin{Bmatrix} \{\eta_{R,I}\} \\ \{\eta_{R,B}\} \\ \{\eta_{R,C}\} \\ \{\eta_{F,B}\} \end{Bmatrix} = \begin{Bmatrix} \{F_{R,I}\} \\ -\{F_{R,B}\} \\ -\{F_{R,C}\} \\ -\{F_{F,B}\} \end{Bmatrix}, \quad (16)$$

$$[Z_{B,BB}] \{\eta_{R,B}\} - [Z_{B,BB}] \{\eta_{F,B}\} = \{F_{B,B}\}, \quad (17)$$

$$- [Z_{B,BB}] \{\eta_{R,B}\} + [Z_{F,FF}] \{\eta_{R,F}\} + [Z_{B,BB}] \{\eta_{F,B}\} = \{F_{F,F}\} \quad (18)$$

and

$$[Z_{C,CC}]_{8 \times 8} \{\eta_{R,C}\}_{8 \times 1} = \{F_{C,CC}\}_{8 \times 1}, \quad (19)$$

where subscripts B , C , F , I and R represent bearing, coupling, foundation, internal and rotor DOFs, respectively. Dynamic matrices may be read as (' $Z_{R,II}$ ' rotor dynamic matrix correspond to internal–internal DOFs, ' $Z_{R,BI}$ ' rotor dynamic matrix correspond to bearing–internal DOFs, ' $Z_{R,BI}$ ' bearing dynamic matrix correspond to bearing–bearing DOFs, etc.). Combining Eqs. (16)–(19), results in system EOMs in frequency domain and could be expressed as

$$\begin{bmatrix} [Z_{R,II}] & [Z_{R,IB}] & [Z_{R,IC}] & [Z_{R,IF}] \\ [Z_{R,BI}] & [Z_{R,BB}] + [Z_{B,BB}] & [Z_{R,BC}] & [Z_{R,BF}] - [Z_{B,BB}] \\ [Z_{R,CI}] & [Z_{R,CB}] & [Z_{R,CC}] + [Z_{C,CC}] & [Z_{R,CF}] \\ [Z_{R,FI}] & [Z_{R,FB}] - [Z_{B,BB}] & [Z_{R,FC}] & [Z_{R,FF}] + [Z_{F,FF}] + [Z_{B,BB}] \end{bmatrix} \begin{pmatrix} \{\eta_{R,I}\} \\ \{\eta_{R,B}\} \\ \{\eta_{R,C}\} \\ \{\eta_{F,B}\} \end{pmatrix} = \begin{pmatrix} \{F_{R,I}\} \\ \{0\} \\ \{0\} \\ \{0\} \end{pmatrix}, \quad (20)$$

where $\{\eta_{R,I}\}$, $\{\eta_{R,B}\}$, $\{\eta_{R,C}\}$ and $\{\eta_{F,B}\}$ are rotor internal, rotor bearing, rotor coupling and foundation bearing DOFs, respectively. Eq. (20), would be used in subsequent section to develop a methodology for the simultaneous estimation of the bearing–coupling–foundation dynamic parameters (BCFDPs) along with residual unbalances (RUs). In the section of numerical experiments, the same equation would be used to get simulated responses for testing the proposed multi-fault identification methodology.

3. Formulation of the quantification methodology

Eq. (20) represents the governing equation for multi-degree of freedom flexible rotor–bearing–coupling–foundation system, considered to develop a methodology to estimate the BCFDPs along with RUs. Eq. (20), could be split and rearranged to

eliminate internal DOFs ($\eta_{R,I}$) from EOMs as

$$\begin{bmatrix} [Z_{B,BB}]_{8 \times 8} & [0]_{8 \times 8} & [-Z_{B,BB}]_{8 \times 8} \\ [0]_{8 \times 8} & [Z_{C,CC}]_{8 \times 8} & [0]_{8 \times 8} \\ [-Z_{B,BB}]_{8 \times 8} & [0]_{8 \times 8} & [Z_{B,BB}]_{8 \times 8} + [Z_{F,FF}]_{8 \times 8} \end{bmatrix}_{(24 \times 24)} \begin{Bmatrix} \eta_{R,B} \\ \eta_{R,C} \\ \eta_{F,B} \end{Bmatrix}_{(24 \times 1)} + \begin{bmatrix} [Z_{R,BI}][Z_{R,II}]^{-1} \\ [Z_{R,CI}][Z_{R,II}]^{-1} \\ [Z_{R,FI}][Z_{R,II}]^{-1} \end{bmatrix}_{(24 \times 32)} \{F_{R,I}\}_{(32 \times 1)} = \begin{Bmatrix} P_{n_1} \\ P_{n_2} \\ P_{n_3} \end{Bmatrix}_{(24 \times 1)}, \quad (21)$$

where

$$\begin{aligned} \{P_{n_1}\} &= \left([Z_{R,IB}] [Z_{R,II}]^{-1} [Z_{R,BI}] - [Z_{R,BB}] \right) \{\eta_{R,B}\} + \\ &\quad \left([Z_{R,BI}] [Z_{R,II}]^{-1} [Z_{R,IC}] - [Z_{R,BC}] \right) \{\eta_{R,C}\} + \\ &\quad \left([Z_{R,BI}] [Z_{R,II}]^{-1} [Z_{R,IF}] - [Z_{R,BF}] \right) \{\eta_{F,B}\}, \\ \{P_{n_2}\} &= \left([Z_{R,CI}] [Z_{R,II}]^{-1} [Z_{R,IB}] - [Z_{R,CB}] \right) \{\eta_{R,B}\} + \\ &\quad \left([Z_{R,CI}] [Z_{R,II}]^{-1} [Z_{R,IC}] - [Z_{R,CC}] \right) \{\eta_{R,C}\} + \\ &\quad \left([Z_{R,CI}] [Z_{R,II}]^{-1} [Z_{R,IF}] - [Z_{R,CF}] \right) \{\eta_{F,B}\}, \\ \{P_{n_3}\} &= \left([Z_{R,FI}] [Z_{R,II}]^{-1} [Z_{R,IB}] - [Z_{R,FB}] \right) \{\eta_{R,B}\} + \\ &\quad \left([Z_{R,FI}] [Z_{R,II}]^{-1} [Z_{R,IC}] - [Z_{R,FC}] \right) \{\eta_{R,C}\} + \\ &\quad \left([Z_{R,FI}] [Z_{R,II}]^{-1} [Z_{R,IF}] - [Z_{R,FF}] \right) \{\eta_{F,B}\}, \\ \{F_{R,I}\} &= \omega^2 [T]_{32 \times 8} \{U\}_{8 \times 1} \end{aligned}$$

with

$$\begin{aligned} T_{31} &= 1, \quad T_{32} = j, \quad T_{41} = -j, \quad T_{42} = 1, \quad T_{11,3} = 1, \quad T_{11,4} = j, \quad T_{12,3} = -j, \quad T_{12,4} = 1, \\ T_{19,5} &= 1, \quad T_{19,6} = j, \quad T_{20,5} = -j, \quad T_{20,6} = 1, \quad T_{27,7} = 1, \quad T_{27,8} = j, \quad T_{28,7} = -j, \quad T_{28,8} = 1, \end{aligned}$$

$$\{U\}_{8 \times 1} = \left\{ u_{x_1}^r \quad u_{x_1}^i \quad u_{x_2}^r \quad u_{x_2}^i \quad u_{x_3}^r \quad u_{x_3}^i \quad u_{x_4}^r \quad u_{x_4}^i \right\}^T,$$

where $[T]$ is transformation matrix, rest of the elements of the transformation matrix is zero. Superscripts r and i represent the real and imaginary parts, respectively. Rearrangement of Eq. (21), could be expressed as

$$[W_N]_{24 \times 74} \{\beta\}_{74 \times 1} + [R_N]_{24 \times 8} \{U\}_{8 \times 1} = \{P_N\}_{24 \times 1}. \quad (22)$$

Here all the unknowns (stiffness and damping parameters of bearing, coupling and foundation and unbalance) are arranged in vector $\{\beta\}$ and $\{U\}$, respectively.

Matrices $[W]$ and $[R]$ contains the response parameters corresponding to stiffness and damping and unbalance, respectively. Separating real and imaginary parts, Eq. (22) could be written as

$$\begin{bmatrix} [W_N^r] \\ [W_N^i] \end{bmatrix}_{48 \times 72} \{\beta\}_{72 \times 1} + \begin{bmatrix} [R_N^r] \\ [R_N^i] \end{bmatrix}_{48 \times 8} \{u\}_{8 \times 1} = \begin{Bmatrix} \{P_N^R\} \\ \{P_N^i\} \end{Bmatrix}_{48 \times 1}, \quad (23)$$

$$[W]_{48 \times 74} \{\beta\}_{74 \times 1} + [R]_{48 \times 8} \{U\}_{8 \times 1} = \{P\}_{48 \times 1}, \quad (24)$$

$$[[W]_{48 \times 74} \quad [R]_{48 \times 8}] \begin{Bmatrix} \{\beta\}_{74 \times 1} \\ \{U\}_{8 \times 1} \end{Bmatrix} = \{P\}_{48 \times 1}, \quad (25)$$

$$[A]_{48 \times 82} \{X\}_{82 \times 1} = \{P\}_{48 \times 1} \quad (26)$$

with

$$\{X\} = \left\{ \begin{array}{l} k_{xx}^{b1}, k_{xy}^{b1}, k_{yx}^{b1}, k_{yy}^{b1}, k_{xx}^{b2}, k_{xy}^{b2}, k_{yx}^{b2}, k_{yy}^{b2}, k_{xx}^{b3}, k_{xy}^{b3}, k_{yx}^{b3}, k_{yy}^{b3}, k_{xx}^{b4}, k_{xy}^{b4}, \\ k_{yx}^{b4}, k_{yy}^{b4}, k_{xx}^c, k_{xy}^c, k_{yx}^c, k_{yy}^c, k_{\varphi x}^c, k_{\varphi y}^c, k_{xx}^{f1}, k_{xy}^{f1}, k_{yx}^{f1}, k_{yy}^{f1}, k_{xx}^{f2}, k_{xy}^{f2}, \\ k_{yx}^{f2}, k_{yy}^{f2}, k_{xx}^{f3}, k_{xy}^{f3}, k_{yx}^{f3}, k_{yy}^{f3}, k_{xx}^{f4}, k_{xy}^{f4}, k_{yx}^{f4}, k_{yy}^{f4}, c_{xx}^{b1}, c_{xy}^{b1}, c_{yx}^{b1}, c_{yy}^{b1}, \\ c_{xx}^{b2}, c_{xy}^{b2}, c_{yx}^{b2}, c_{yy}^{b2}, c_{xx}^{b3}, c_{xy}^{b3}, c_{yx}^{b3}, c_{yy}^{b3}, c_{xx}^{b4}, c_{xy}^{b4}, c_{yx}^{b4}, c_{yy}^{b4}, c_{xx}^c, c_{xy}^c, c_{yx}^c, \\ c_{yy}^c, c_{xx}^{f1}, c_{xy}^{f1}, c_{yx}^{f1}, c_{yy}^{f1}, c_{xx}^{f2}, c_{xy}^{f2}, c_{yx}^{f2}, c_{yy}^{f2}, c_{xx}^{f3}, c_{xy}^{f3}, c_{yx}^{f3}, c_{yy}^{f3}, \\ c_{xx}^{f4}, c_{xy}^{f4}, c_{yx}^{f4}, c_{yy}^{f4}, u_{x1}^r, u_{x1}^i, u_{x2}^r, u_{x2}^i, u_{x3}^r, u_{x3}^i, u_{x4}^r, u_{x4}^i \end{array} \right\}.$$

Eq. (26) is the final form of regression equation where all the unknowns are stacked in the left side in column vector $\{X\}$. $[A]$ is combined regression matrix having the effect of stiffness, damping and residual unbalance. From Eq. (26), it could be seen that this is the case of the underdetermined system of linear simultaneous equations in which number of unknowns (eighty two) are more than the number of equations (forty eight). The complete unknowns could be estimated by increasing the number of equation at least equal to or greater than the number of unknowns. For the present case, to avoid undermined condition, at least two sets of independent measurements are required. The advantage of current methodology is that it needs only linear DOFs at bearing, coupling and foundation locations and few angular DOFs at coupling location that are practically measurable quantities. To obtain independent sets of measurement two different groups have been suggested [16]:

Group A: Run the rotor in same sense at unlike speeds.

Group B: Run the rotor in CW (clockwise) and CCW (counter clockwise) directions, alternatively at alike or unlike spin speed. It is assumed that the bearing, coupling and foundation parameters do not change with the speed.

Under these techniques, three different methods have been proposed:

Method I: Run the rotor near critical speeds (i.e., near and outside the half power points. Half power points are the two frequencies on both sides of the resonance. Frequency on either side is referred as sideband which is equal to $0.707X_{res}$ where X_{res} is the resonant amplitude).

Method II: Run the rotor away from the critical speeds.

Method III: Run the rotor at several speeds.

Eq. (25), could be rewritten for two different groups to estimate BCFDPs and RUs of the system as

Group A:

$$[A_I]_{96 \times 82} \{X_I\}_{82 \times 1} = \{P_I\}_{96 \times 1} \quad (27)$$

with

$$[A_I]_{96 \times 82} = \begin{bmatrix} A(\omega_1)_{48 \times 82} \\ A(\omega_2)_{48 \times 82} \end{bmatrix}; \quad [P_I]_{96 \times 82} = \begin{bmatrix} P(\omega_1)_{48 \times 82} \\ P(\omega_2)_{48 \times 82} \end{bmatrix},$$

where $[A_I]$ and $[P_I]$ are similar in the formulation as in Eq. (25), with unlike spin speeds. Eq. (26), is the standard form of regression equation for *Group A* used to obtain BCFDPs and RUs with the help of least-squares fit as

$$\{X_I\}_{82 \times 1} = \left([A_I(\omega)]'_{82 \times 96} [A_I(\omega)]_{96 \times 82} \right)^{-1} [A_I(\omega)]'_{82 \times 96} \{P_I(\omega)\}_{96 \times 1}. \quad (28)$$

Group B:

$$[A_{II}]_{48 \times 82} \{X_{II}\}_{82 \times 1} = \{P_{II}\}_{48 \times 1} \quad (29)$$

with

$$[A_{II}]_{96 \times 82} = \begin{bmatrix} A(\omega_1)_{48 \times 82} \\ A(-\omega_1)_{48 \times 82} \end{bmatrix}; \quad [P_{II}]_{96 \times 82} = \begin{bmatrix} P(\omega_1)_{48 \times 82} \\ P(-\omega_1)_{48 \times 82} \end{bmatrix},$$

where $[A_{II}]$ and $[P_{II}]$ are similar in the formulation as in Eq. (25), with unlike spin speeds. Eq. (28), is the standard form of regression equation for *Group B* used to obtain BCFDPs and RUs with the help of least-squares fit as

$$\{X_{II}\}_{82 \times 1} = \left([A_{II}(\omega)]'_{82 \times 96} [A_{II}(\omega)]_{96 \times 82} \right)^{-1} [A_{II}(\omega)]'_{82 \times 96} \{P_{II}(\omega)\}_{96 \times 1}. \quad (30)$$

From Eq. (27) and (29), it could be seen that estimation of parameters require inversion of regression matrix, i.e., $\left([A_I(\omega)]'_{82 \times 96} [A_I(\omega)]_{96 \times 82} \right)^{-1} \approx 0$ and $\left([A_{II}(\omega)]'_{82 \times 96} [A_{II}(\omega)]_{96 \times 82} \right)^{-1} \approx 0$, respectively. The accuracy of estimated parameters highly depends on the condition of the regression matrix to be inverted. To avoid ill-conditioning of regression matrix, column scaling (the columns corresponding to damping and unbalance parameters are divided by the average of spin speed (ω_{av}) considered) has been performed for three methods suggested under two groups namely **Group A** and **Group B**.

4. Numerical experiments

To explain the present developed algorithm, fully assembled turbogenerator system is considered (refer Fig. 1). Both shafts have same physical (diameter, length) and mechanical (density, modulus of elasticity) properties as 0.02 m, 1.25 m, 7800 kg/m³ and 2.1×10^9 N/m², respectively. To obtain the simulated response required for developed identification methodology stiffness and damping parameters of bearing, coupling and foundation along with residual unbalance are assumed.

A typical variation of response (linear displacement at bearing 1) with respect to spin speed is shown in Fig. 3a and Fig. 3b, for without and with foundation, respectively. From Fig. 3a, first six critical frequencies of the system (without consideration of foundation) could be noted as $\omega_{cr1} = 160$ rad/s, $\omega_{cr2} = 210$ rad/s, $\omega_{cr3} = 290$ rad/s, $\omega_{cr4} = 360$ rad/s, $\omega_{cr5} = 650$ rad/s, and $\omega_{cr6} = 1170$ rad/s. It could be noted that, after incorporating foundation in the system, critical frequencies are slightly varying refer Fig. 3b, these phenomenon is also reported in [22]. The present identification methodology (Eq. (27) and (29)) requires forced response data to estimate BCFDPs along with RUs for two different groups as discussed above, i.e., **Group A** and **Group B**, respectively. In the subsequent sub-section percentage deviation in estimation is compared with assumed values for different methods discussed above. The percentage deviation is calculated as

$$\% \text{ Deviation} = \frac{\text{Assumed value} - \text{Estimated value}}{\text{Assumed value}} \times 100.$$

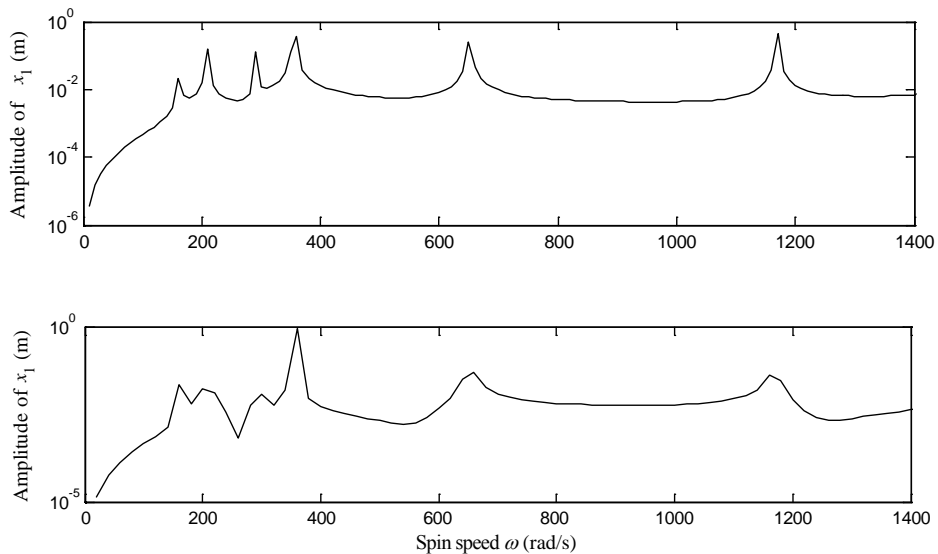


Fig. 3. Horizontal displacement at bearing location 1 (a) without foundation (b) with foundation

Column scaling of regression matrices $[A_I]$ and $[A_{II}]$ has been performed to enhance the correctness of the estimated parameters. To have an idea of the effect of column scaling, the comparison of percentage deviation in estimated parameter before and after column scaling is performed. For example, the effect of column scaling for **Method I, II and III** under **Group A** is reported in this article for 1% measurement noise in Fig. 4, Fig. 5 and Fig. 6, respectively. An appreciable improvement in estimated parameters after column scaling could be observed from Figs 4–6. Also, it could be observed that the maximum percentage deviation occurred prior to column scaling for **Method I, II and III** under **Group A** for

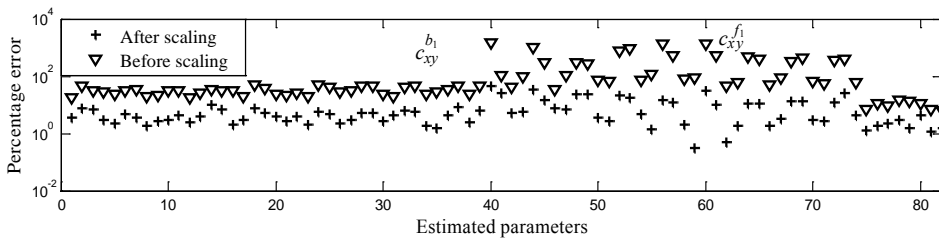


Fig. 4. Percentage deviation in estimated parameters before and after column scaling for Method I of Group A (for 1% measurement noise)

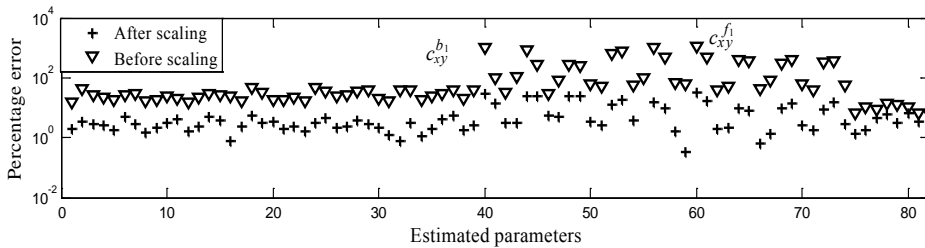


Fig. 5. Percentage deviation in estimated parameters before and after column scaling for Method II of Group A (for 1% measurement noise)

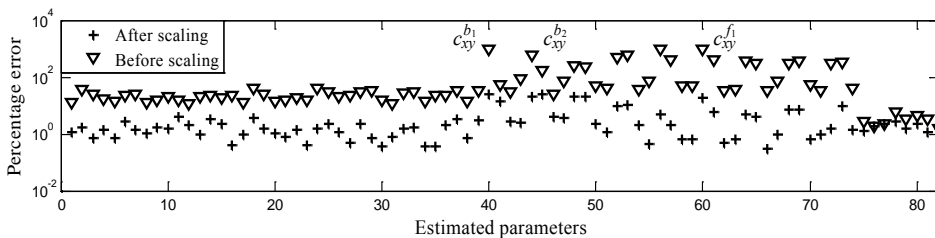


Fig. 6. Percentage deviation in estimated parameters before and after column scaling for Method III of Group A (for 1% measurement noise)

1% measurement noise is 1460%, 1168%, 986%, which is considerably decreased after the column scaling, i.e., 45%, 32%, 31%, respectively. In Figs 4–13, the number in the abscissa represents estimated parameter i.e., vector $\{X\}$ of Eq. (26). Another significant effect of column scaling is an improvement in condition number presented in Table 1.

4.1. Group A: Run the rotor in same sense at unlike speeds

Method I: The two speeds selected near the critical speeds, however, outside the half-power point to generate independent sets of measurement are $\omega_1 = 145$ rad/s and $\omega_2 = 175$ rad/s. Generated response is used to estimate BCFDPs along with RUs. From Fig. 7, it could be observed that most of the identified parameters exhibit deviation with assumed values for 1% measurement noise and the variation increases as the percentage noise increases. From Table 1, the improvement in the condition number after column scaling of the order of 10^{16} could be observed. From Table 2, it could be observed that the maximum error occurred in cross-coupling damping parameter of the bearing is 45% and 113% for 1% and 5% measurement noise, respectively.

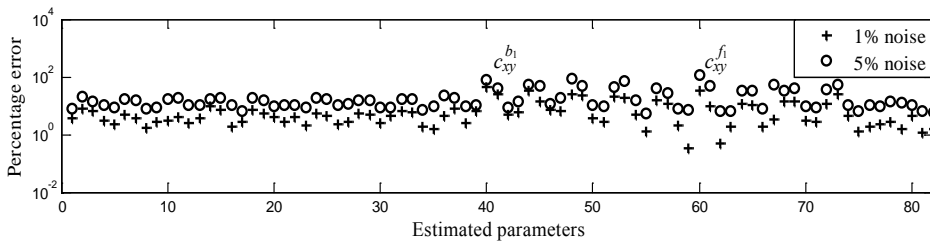


Fig. 7. Percentage deviation in estimated parameters for different level of measurement noise for Method I of Group A

Method II: The two speeds selected away from critical speeds to generate independent sets of measurement are $\omega_1 = 110$ rad/s and $\omega_2 = 245$ rad/s. From Fig. 8, it could be seen that most of the bearing parameters are showing good agreement for 1% measurement and varying slightly for 5% noise. Damping parameters

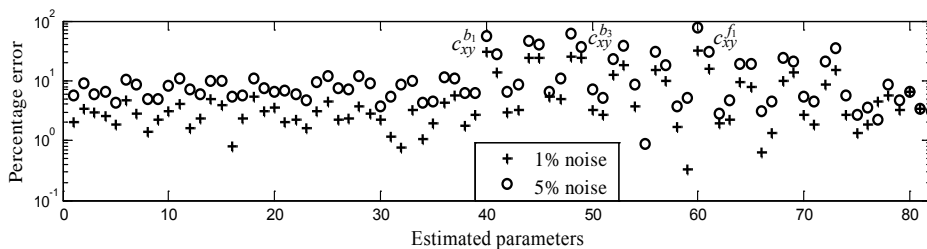


Fig. 8. Percentage deviation in estimated parameters for different level of measurement noise for Method II of Group A

Summary of improvement in condition number for different methods

Table 1.

| Groups | Methods | Order of condition number | | | Order of improvement in condition number | |
|----------------|-------------------|---------------------------|--------------|--------------|--|--------------|
| | | Before column scaling | For 5% noise | For 1% noise | For 1% noise | For 5% noise |
| Group A | <i>Method I</i> | 10^{28} | 10^{28} | 10^{12} | 10^{12} | 10^{16} |
| | <i>Method II</i> | 10^{28} | 10^{28} | 10^{12} | 10^{12} | 10^{16} |
| | <i>Method III</i> | 10^{28} | 10^{28} | 10^{11} | 10^{11} | 10^{17} |
| Group B | <i>Method I</i> | 10^{27} | 10^{27} | 10^{10} | 10^{10} | 10^{17} |
| | <i>Method II</i> | 10^{27} | 10^{27} | 10^9 | 10^9 | 10^{18} |
| | <i>Method III</i> | 10^{27} | 10^{27} | 10^6 | 10^6 | 10^{21} |

Summary of estimated parameters having maximum percentage error for different methods

Table 2.

| Groups | Methods | Estimated parameters with max. % deviation | | | % reduction in error on estimates after column scaling | |
|----------------|-------------------|--|-----------------------|---------------------|--|--------------|
| | | For 1% noise | For 5% noise | For 1% noise | For 1% noise | For 5% noise |
| Group A | <i>Method I</i> | $c_{xy}^{B_1}$ (1460) | $c_{xy}^{B_1}$ (1742) | $c_{xy}^{B_1}$ (45) | $c_{xy}^{B_1}$ (113) | 96.92 |
| | <i>Method II</i> | $c_{xy}^{F_1}$ (1168) | $c_{xy}^{F_1}$ (1321) | $c_{xy}^{F_1}$ (32) | $c_{xy}^{F_1}$ (77) | 97.62 |
| | <i>Method III</i> | $c_{xy}^{F_1}$ (986) | $c_{xy}^{F_1}$ (1081) | $c_{xy}^{F_1}$ (31) | $c_{xy}^{F_1}$ (50) | 96.86 |
| Group B | <i>Method I</i> | $c_{xy}^{F_1}$ (95) | $c_{xy}^{F_1}$ (233) | $c_{xy}^{F_1}$ (28) | $c_{xy}^{F_1}$ (95) | 70.53 |
| | <i>Method II</i> | $c_{xy}^{F_1}$ (79) | $c_{xy}^{F_1}$ (137) | $c_{xy}^{F_1}$ (20) | $c_{xy}^{F_1}$ (40) | 74.68 |
| | <i>Method III</i> | $c_{xy}^{F_1}$ (39) | $c_{xy}^{F_1}$ (68) | $c_{xy}^{F_1}$ (6) | $c_{xy}^{F_1}$ (13) | 84.62 |

start deviating even at 1% measurement noise. From Table 1, the improvement in the condition number after column scaling of the order of 10^{16} could be observed. From Table 2, it could be concluded that **Method II** is better than **Method I** under **Group A** to estimate the parameters. Cross-coupled damping parameter of foundation occur maximum deviation in this case as 32% and 77% for 1% and 5% measurement noise, respectively.

Method III: The number of measurement speed to generate a response is increased up to 300 in numbers, i.e., $\omega = 0\text{--}1500$ rad/s with an interval of 5 rad/s to estimate the parameters. From Fig. 9, it could be observed that most of the parameters (except bearing and foundation damping parameters) show good agreement with assumed values up to 5% measurement noise. From Table 2, it could be seen that cross-coupled damping parameters of foundation show maximum deviation 31% and 50% for 1% and 5% measurement noise, respectively. From Table 1 and Table 2 and by comparing Figs 7–9, it could be observed that **Method III** is the best method to estimate the parameters under **Group A**.

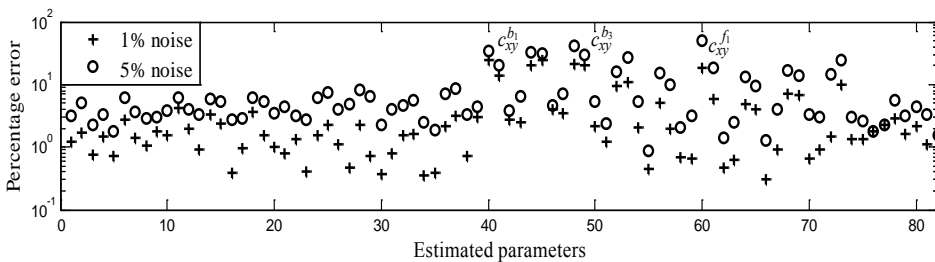


Fig. 9. Percentage deviation in estimated parameters for different level of measurement noise for Method III of Group A

4.2. Technique 2: Run the rotor alternately in unlike direction (i.e., CW and CCW)

From different methods discussed under **Group A**, it could be observed that the estimated parameters show deviation with assumed parameters even at 1% measurement noise and increases as the level of measurement noise increases. To improve the closeness of developed methodology **Group B** is proposed where response is generated by running the rotor alternatively in unlike, i.e., (CW and CCW) directions.

Method I: The two speeds selected near the critical speeds however outside the half-power point to generate independent sets of measurement are $\omega_1 = 145$ rad/s (for CW) and $\omega_1 = 145$ rad/s (for CCW). Generated response is used to estimate BCFDPs along with RUs. From Fig. 10, it could be observed that most of the identified parameters exhibit good agreement with assumed values up to 5% measurement noise. Some of the damping parameters mainly cross-coupled damping

parameters of foundation show deviation at 5% measurement noise. From Table 1, it could be observed that the condition number after column scaling is enhanced by the order of 10^{16} . From Table 2, it could be observed that the maximum error occurred in cross-coupling damping parameter of the foundation is 28% and 95% for 1% and 5% measurement noise, respectively.

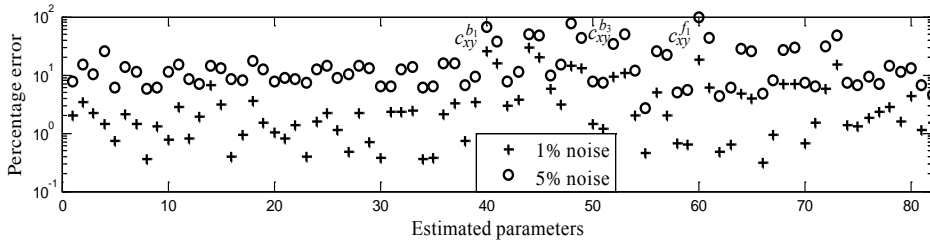


Fig. 10. Percentage deviation in estimated parameters for different level of measurement noise for Method I of Group B

Method II: The two speeds selected away from critical speeds to generate independent sets of measurement are $\omega_1 = 110$ rad/s (for CW) and $\omega_1 = 110$ rad/s (for CCW). From Fig. 11, it could be observed that most of the parameters (except few bearing and foundation damping parameters) show good agreement with assumed values up to 5% measurement noise. The maximum deviation occurred for the aforementioned case is 20% and 40% for 1% and 5% measurement noise, respectively (refer Table 2). From Table 1, it could be observed that the condition number after column scaling is enhanced by the order of 10^{18} .

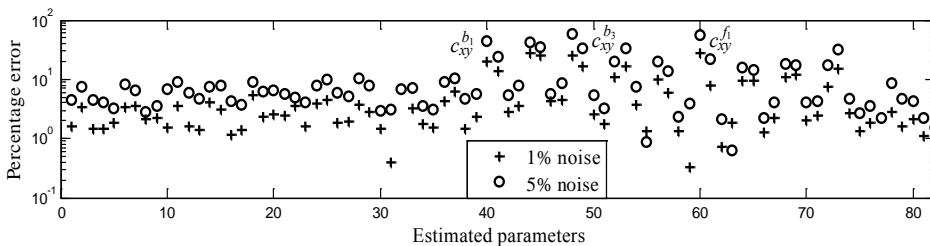


Fig. 11. Percentage deviation in estimated parameters for different level of measurement noise for Method II of Group B

Method III: The number of measurement speed to generate a response is increased up to 300 in numbers, i.e., for CW $\omega = 0-1500$ rad/s and for CCW $\omega = 0-1500$ rad/s with an interval of 10 rad/s to estimate the parameters. From Fig. 12, it could be observed that all the parameters are identified well and show good agreement with assumed values up to 5% measurement noise. From Fig. 12,

it could be seen that the maximum error occurred, in this case, is 6% and 13% for 1% and 5% measurement noise, respectively. From Table 1, the improvement in the condition number after column scaling of the order of 10^{21} could be observed that is a maximum improvement under both the groups and all three methods. By comparing Figs 7–12 and from Table 2, it could be observed that **Method III** under **Group B** is the best method to estimate the parameters among both the groups.

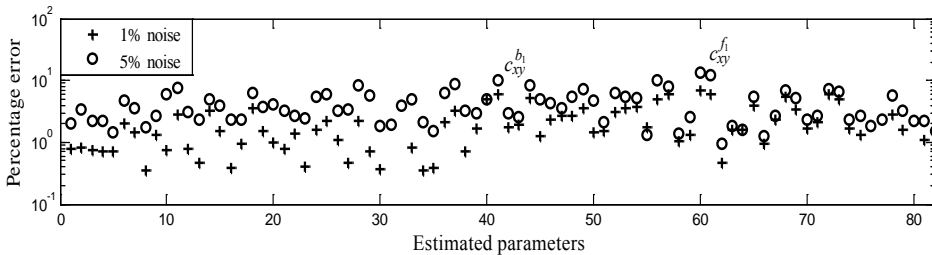


Fig. 12. Percentage deviation in estimated parameters for different level of measurement noise for Method III of Group B

The effect of modelling error on the developed algorithm is carried out for best-estimated method (i.e., **Method III** under **Group B**) and shown in Fig. 13. The effect of modelling error is consider by considering 5% deviation in modulus of elasticity (E) and the density (ρ) for 5% measurement noise. From Fig. 13, it is clear that the algorithm is robust against modelling error and show well agreement with estimated parameters obtained for **Method III** under **Group B** for 5% measurement noise. A comparison of response (horizontal displacement at bearing location 1) generated from assumed values of parameters (i.e., true model) and estimated values of parameters (i.e., identified model) for **Method III** of **Group B** for 5% measurement noise condition is presented in Fig. 14. From Fig. 14, it could be concluded that the response obtained from true model and estimated model exhibit well agreement with each other.

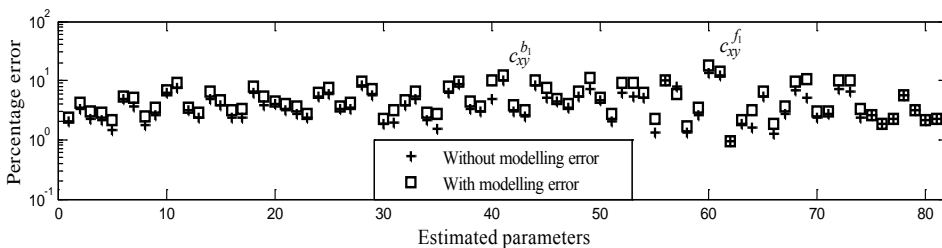


Fig. 13. Percentage deviation in estimated parameters for 5% variation in E and ρ for Method III of Group B (for 5% measurement noise)

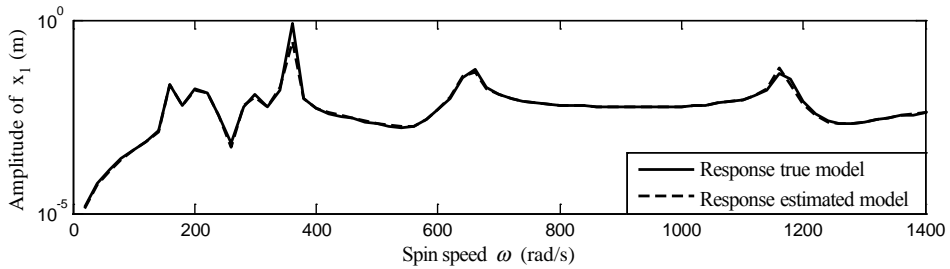


Fig. 14. Comparison of horizontal response at bearing location 1 for true model and estimated model under Method III of Group B for 5% measurement noise

5. Conclusions

A quantification methodology based on least squares fit technique by using forced response data system is developed in this article. The most common faults that exist in turbine generator system, i.e., bearing fault, coupling misalignment and foundation are successfully identified regarding their dynamic parameters. The advantage of present identification methodology is in twofold: first, it requires measurement at practically measurable and accessible locations, second, any number of bearings, couplings, foundations, and rotor could be incorporated in the system. An identification algorithm is developed in the MATLAB^R2012b environment on HP build CPU with 4GB RAM and core i7 processor. The developed methodology is analyzed for the different level of measurement noise and modeling error in the system and found to be robust. A different method was proposed and implemented to improve the conditioning of the regression matrix, and it is observed that the improvement in the condition number plays a vital role in the accuracy of estimated parameters. Since the least squares fitting approach is speedy due to its mathematical simplicity, it could be used to validate the proposed methodology in a laboratory test rig and an actual machine along with this, some other identification technique such as Kalman Filter could be used as an identification algorithm to estimate the parameters, in future.

Manuscript received by Editorial Board, November 20, 2017;
final version, February 14, 2018.

References

- [1] R.A. Collacott. *Mechanical fault diagnosis and condition monitoring*. Chapman & Hall, 1977.
- [2] J.S. Mitchell. *An introduction to machinery analysis and monitoring*.: Pennwell Corp., Tulsa, Oklahoma, 1993.
- [3] S. Edwards, A.W. Lees, and M.I. Friswell. Fault diagnosis of rotating machinery. *Shock and Vibration Digest*, 30(1):4–13, 1998.

- [4] R. Tiwari. Conditioning of regression matrices for simultaneous estimation of the residual unbalance and bearing dynamic parameters. *Mechanical Systems and Signal Processing*, 19(5):1082–1095, 2005. doi: [10.1016/j.ymsp.2004.09.005](https://doi.org/10.1016/j.ymsp.2004.09.005).
- [5] A.W. Lees, J.K. Sinha, and M.I. Friswell. Model-based identification of rotating machines. *Mechanical Systems and Signal Processing*, 23(6):1884–1893, 2009. doi: [10.1016/j.ymsp.2008.08.008](https://doi.org/10.1016/j.ymsp.2008.08.008).
- [6] D.J. Bordoloi and R. Tiwari. Optimum multi-fault classification of gears with integration of evolutionary and SVM algorithms. *Mechanism and Machine Theory*, 73:49–60, 2014. doi: [10.1016/j.mechmachtheory.2013.10.006](https://doi.org/10.1016/j.mechmachtheory.2013.10.006).
- [7] A.S. Sekhar and B.S. Prabhu. Effects of coupling misalignment on vibrations of rotating machinery. *Journal of Sound and Vibration*, 185(4):655–671, 1995. doi: [10.1006/jsvi.1995.0407](https://doi.org/10.1006/jsvi.1995.0407).
- [8] M.G. Smart, M.I. Friswell, and A.W. Lees. Estimating turbogenerator foundation parameters: model selection and regularization. *Proceedings of the Royal Society A: Mathematical, Physical and Engineering Sciences*, 456(1999):1583–1607, 2000. doi: [10.1098/rspa.2000.0577](https://doi.org/10.1098/rspa.2000.0577).
- [9] R. Provasi, G.A. Zanetta, and A. Vania. The extended Kalman filter in the frequency domain for the identification of mechanical structures excited by sinusoidal multiple inputs. *Mechanical Systems and Signal Processing*, 14(3):327–341, 2000. doi: [10.1006/mssp.1999.1259](https://doi.org/10.1006/mssp.1999.1259).
- [10] N. Feng and E.J. Hahn. Numerical evaluation of an identification technique for flexibly supported rigid turbomachinery foundations. *Australian Journal of Mechanical Engineering*, 1(2):73–82, 2004. doi: [10.1080/14484846.2004.11464469](https://doi.org/10.1080/14484846.2004.11464469).
- [11] P. Pennacchi, N. Bachschmid, A. Vania, G.A. Zanetta, and L. Gregori. Use of modal representation for the supporting structure in model-based fault identification of large rotating machinery: part 1 – theoretical remarks. *Mechanical Systems and Signal Processing*, 20(3):662–681, 2006. doi: [10.1016/j.ymsp.2004.11.006](https://doi.org/10.1016/j.ymsp.2004.11.006).
- [12] P. Pennacchi, N. Bachschmid, A. Vania, G.A. Zanetta, and L. Gregori. Use of modal representation for the supporting structure in model-based fault identification of large rotating machinery: Part 2 – application to a real machine. *Mechanical Systems and Signal Processing*, 20(3):682–701, 2006. doi: [10.1016/j.ymsp.2004.12.005](https://doi.org/10.1016/j.ymsp.2004.12.005).
- [13] Y.S. Chen, Y.D. Cheng, T. Yang, and K.L. Koai. Accurate identification of the frequency response functions for the rotor–bearing–foundation system using the modified pseudo mode shape method. *Journal of Sound and Vibration*, 329(6):644–658, 2010. doi: [10.1016/j.jsv.2009.09.038](https://doi.org/10.1016/j.jsv.2009.09.038).
- [14] A. Heng, S. Zhang, A.C. Tan, and J. Mathew. Rotating machinery prognostics: State of the art, challenges and opportunities. *Mechanical Systems and Signal Processing*, 23(3):724–739, 2009. doi: [10.1016/j.ymsp.2008.06.009](https://doi.org/10.1016/j.ymsp.2008.06.009).
- [15] K.L. Cavalca and E.P. Okabe. On the analysis of rotor–bearing–foundation systems. *Proceedings of the IUTAM Symposium on Emerging Trends in Rotor Dynamics*, New Delhi, 23–26 March, 2009, pp. 89–101, Springer 2011. doi: [10.1007/978-94-007-0020-8_8](https://doi.org/10.1007/978-94-007-0020-8_8).
- [16] M. Lal and R. Tiwari. Multi-fault identification in simple rotor–bearing–coupling systems based on forced response measurements. *Mechanism and Machine Theory*, 51:87–109, 2012. doi: [10.1016/j.mechmachtheory.2012.01.001](https://doi.org/10.1016/j.mechmachtheory.2012.01.001).
- [17] M. Lal and R. Tiwari. Quantification of multiple fault parameters in flexible turbo-generator systems with incomplete rundown vibration data. *Mechanical Systems and Signal Processing*, 41(1–2):546–563, 2013. doi: [10.1016/j.ymsp.2013.06.025](https://doi.org/10.1016/j.ymsp.2013.06.025).
- [18] Y. Lei, J. Lin, Z. He, and M.J. Zuo. A review on empirical mode decomposition in fault diagnosis of rotating machinery. *Mechanical Systems and Signal Processing*, 35(1–2):108–126, 2013. doi: [10.1016/j.ymsp.2012.09.015](https://doi.org/10.1016/j.ymsp.2012.09.015).
- [19] M. Yu, N. Feng, and E.J. Hahn. An equation decoupling approach to identify the equivalent foundation in rotating machinery using modal parameters. *Journal of Sound and Vibration*, 365:182–198, 2016. doi: [10.1016/j.jsv.2015.11.039](https://doi.org/10.1016/j.jsv.2015.11.039).

-
- [20] H.D. Nelson. A finite rotating shaft element using Timoshenko beam theory. *ASME, Journal of Mechanical Design*, 102(4):793–803, 1980. doi: [10.1115/1.3254824](https://doi.org/10.1115/1.3254824).
- [21] R.W. Clough and J. Penzien. *Dynamics of Structures*. 2nd edition. New York, McGraw-Hill, 1993.
- [22] K.L. Cavalca, P.F. Cavalcante, and E.P. Okabe. An investigation on the influence of the supporting structure on the dynamics of the rotor system. *Mechanical Systems and Signal Processing*, 19(1):157–174, 2005. doi:[10.1016/j.ymsp.2004.04.001](https://doi.org/10.1016/j.ymsp.2004.04.001).